Ultrastructural Alterations in Allylamine Cardiovascular Toxicity

Late Myocardial and Vascular Lesions

PAUL J. BOOR, MD, and
VICTOR J. FERRANS, MD, PhD

From the Chemical Pathology Division, Department of Pathology, University of Texas Medical Branch, Galveston, Texas; and the Pathology Branch, National Heart, Lung and Blood Institute, National Institutes of Health, Bethesda, Maryland

The late myocardial and vascular ultrastructural changes in rat hearts following consumption of the cardiovascular toxin allylamine were studied. Rats were given 0.1% allylamine HCl in drinking water for 10–104 days. From 10 to 21 days, there was organization of acute myocardial necrosis by macrophages and scattered polymorphonuclear leukocytes with prominent interstitial-cell proliferation. Alterations at 21–104 days included extensive scarring with formation of dense mature collagen with scattered fibroblasts present, grossly evident left-ventricular aneurysm, and gross and microscopic changes similar to those observed in the secondary form of endocardial fibroelastosis. Areas of scar contained highly cellular foci of smooth-muscle cells, myofibroblasts, and abundant extracellular elastin. Cardiac myocytes frequently showed markedly disorganized myofilaments, bizarrely distorted mitochondria with condensed cristae, and other severe degenerative changes. Small vessels within and adjacent to scar showed proliferation of intimal smooth-muscle cells. Endothelial lesions or recent or organized thrombi were not seen. Focal endocardial metaplasia, consisting of both chondroid and osseous tissue, was found in areas of transmural scarring, or ventricular aneurysm. Chondrocytes had the overall nuclear and cellular morphology, abundant rough endoplasmic reticulum, and surrounding lacunae typical of mature fibrocartilage. In some areas, the collagen matrix was undergoing calcification with the typical cross-banded pattern of calcifying connective tissue. Osteocytes were located in a densely calcified bone matrix and displayed characteristic cellular extensions into surrounding canaliculi. These findings indicate a severe myocardial, small-vessel, and endocardial injury during the course of chronic allylamine intoxication. (Am J Pathol 1985, 121:39–54)

IN A PREVIOUS PAPER we characterized the early myocardial ultrastructural alterations which occur in rats given allylamine orally[1]; these alterations consist of acute myocardial necrosis without vascular occlusion, followed by a prompt inflammatory infiltrate composed predominantly of macrophages. Late cardiovascular lesions also occur in several species of animals following the repeated or long-term intravenous, intra-arterial, or oral administration of allylamine. These late alterations include aortic intimal hyperplasia and cartilaginous dysplasia,[2–4] coronary arterial intimal fibrous proliferation[4–7] and medial hyalinosis,[2] and smooth-muscle proliferation in smaller intramyocardial arteries.[8] Perhaps the most remarkable late allylamine-induced lesions, however, are the bizarre myocardial alterations, which include transmural scarring with ventricular aneurysm formation[2,3,9,10] and endocardial cartilaginous metaplasia with calcification, resembling osseous metaplasia.[10]

This study describes the ultrastructure of the late alterations which occur in rats after long-term allylamine administration.

Materials and Methods

Twenty male Sprague–Dawley rats (180–220 g) were allowed free access to 0.1% allylamine HCl as their only

Supported by Research Career Development Award HL00929 and Grant HL26189 from the National Heart, Lung, and Blood Institute.

Accepted for publication May 1, 1985.

Address reprint requests to Paul J. Boor, MD, Department of Pathology, Chemical Pathology Division, University of Texas Medical Branch, Galveston, TX 77550.

1

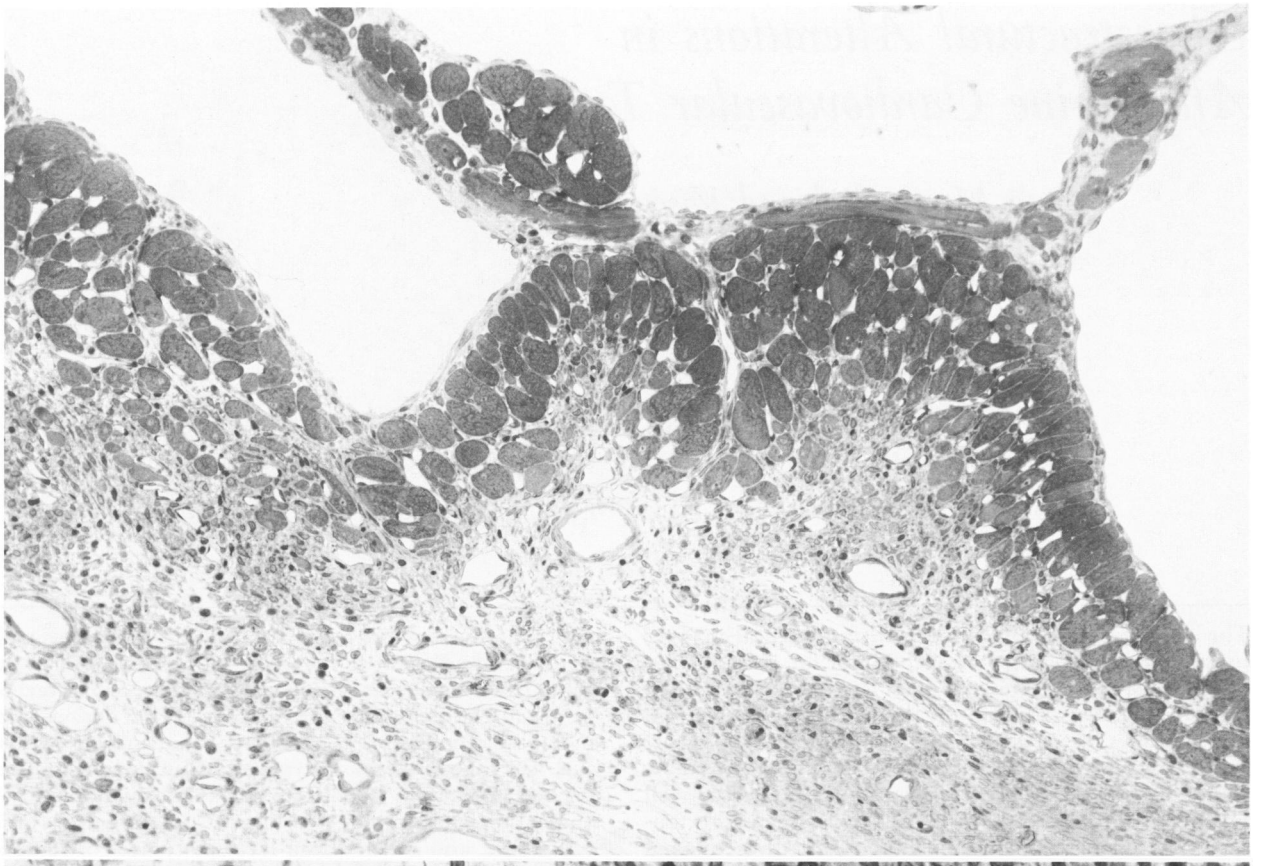

2

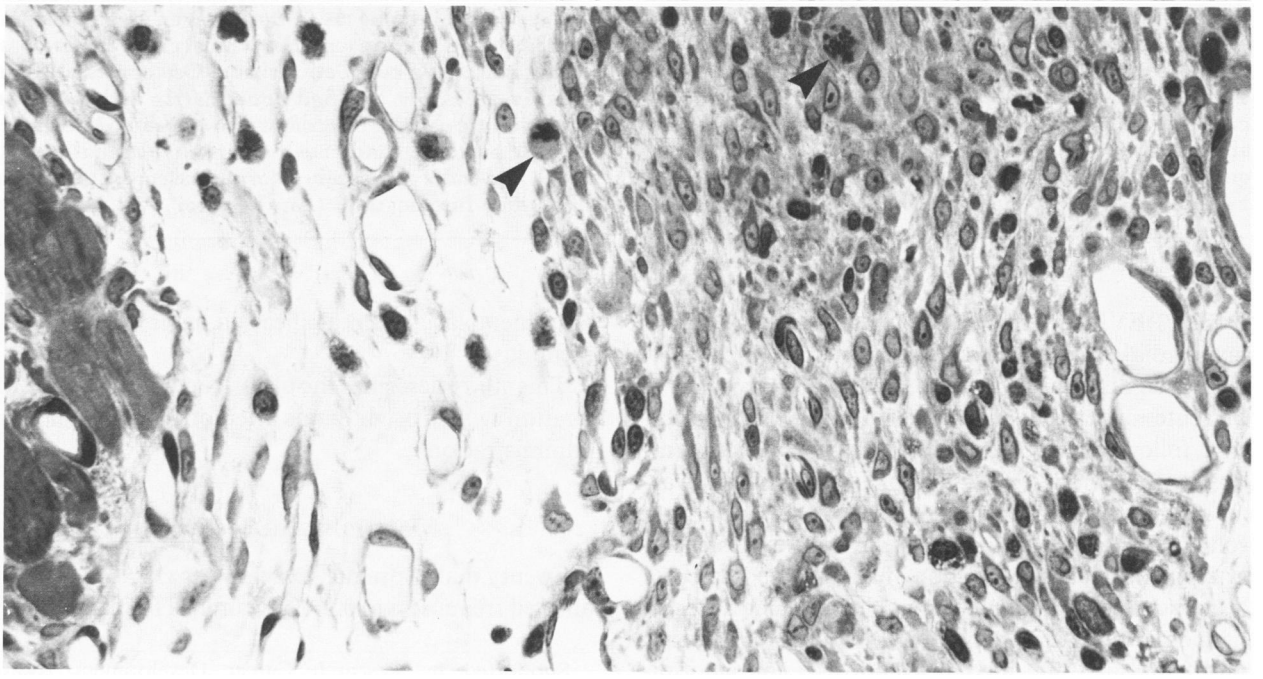

Figure 1—Light micrograph of 1-μ-thick section of rat left-ventricular endocardium shows the organizing myocardial necrosis seen at 10–21 days of allylamine consumption; a diffuse cellular infiltrate is present; necrotic myocytes are not evident. Note the sparing of a layer of myocytes, 2–5 cells thick; a similar spared layer of cells was also present in the epicardium. Ten days of allylamine consumption. (Toluidine blue, ×490) **Figure 2**—Light micrograph of areas of organizing myocardial necrosis shows inflammatory infiltrate of macrophages, a few polymorphonuclear leukocytes, prominent capillaries, and interstitial cells with frequent mitoses (*arrows*). Ten days of allylamine consumption. (Toluidine blue, ×500)

drinking fluid; details of this allylamine protocol have been previously described.[9] Allylamine was consumed for 10–17 days (7 rats), 21–28 days (7 rats), or 90–104 days (6 rats); 6 age-matched control rats were given plain tap water and were killed concurrently with experimental rats. As previously described,[1] rats were anesthetized and sacrificed by perfusion of the heart for 10 minutes with 2% glutaraldehyde in 0.1 M cacodylate buffer (430 mOsm). Grossly evident lesions, consisting of patchy white scars over the ventricles were graded on a severity scale of 1–4 as follows: grade 0, no gross lesions; grade 1, small patches of white scar tissue evident over ventricles; grade 2, multiple scarred areas; grade 3, multiple scarred areas, focally transmural; grade 4, bulging ventricular aneurysm evident.

Hearts were cut transversely into slices of 1–2 mm in thickness and allowed to remain in fixative for 1 hour. Slices were either cut into small 1-mm blocks or processed whole; selected blocks were cut with a jeweler's saw and flat-embedded. Tissue blocks (10–20 per rat) were selected predominantly from areas of myocardium with grossly evident scarring or from firm, white endocardial plaques. Hence, the apex and subendocardial left ventricle were most frequently sampled because these areas show the most extensive gross changes in allylamine-induced cardiomyopathy.[9,10] Tissue was postfixed in 1% osmium tetroxide, dehydrated, and embedded in Epon. One-micron-thick sections of all blocks were cut and stained with toluidene blue for study of the morphologic alterations; selected areas (2–6 blocks per experimental rat; 1 block for each control) were thin-sectioned for electron microscopy, stained with lead citrate and uranyl acetate, and observed in either a Philips EM 200 or a JEOL 100B electron microscope. Selected thin sections were stained by the electron-microscopic elastic tissue technique of Kajikawa et al.[11]

Additional hearts from 11 rats consuming allylamine for 21 or 104 days were fixed in 10% neutral buffered formalin, cut perpendicular to their long axis into 5–8 slices, and routinely dehydrated and embedded in paraffin. Sections were cut and stained by Masson's trichrome and Verhoeff-van Gieson elastic tissue techniques for assessment of scarred areas of myocardium. Also, for gross photography, the left ventricular free wall was dissected free from a heart which displayed characteristic scarring in a separate rat that consumed allylamine for 90 days.

Results

Evolving Necrosis

Areas of acute myocardial necrosis undergoing organization were characterized grossly by thinned, pur-

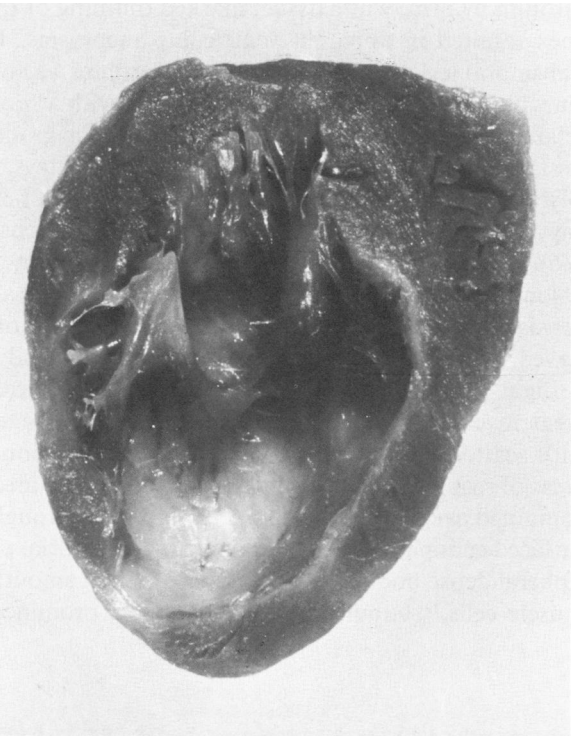

Figure 3—Left-ventricular free wall shows transmural scarring with markedly thinned ventricular wall (aneurysm) and a firm, white, glistening endocardial surface with a procelain-like appearance; such areas frequently contain abundant elastin and cartilaginous and osseous metaplasia. This and all subsequent micrographs are from rats consuming allylamine for 90 days. (Formalin fixation, ×12)

plish areas of myocardium and were seen in rats given allylamine for 10–17 days. By light and electron microscopy these areas consisted of remnants of necrotic myocytes associated with an inflammatory infiltrate of macrophages with scattered polymorphonuclear leukocytes, interstitial cells frequently undergoing mitosis, and prominent capillaries (Figures 1 and 2). A layer of myocytes, 2–5 cells thick, was generally spared in the immediate subendocardium and subepicardium in areas with transmural involvement (Figure 1). Individual myocytes and small groups of myocytes were occasionally noted to be undergoing acute myocardial necrosis at all times examined; necrosis was of the myofibrillar degeneration and contraction band type, as previously detailed.[1]

Mural Scarring

Rats given allylamine for 21–28 or 90–104 days showed grossly evident myocardial scarring which involved the left ventricular apex, free wall, and interventricular septum most frequently, but also was noted in the right ventricle. Scars were characterized by thinning of the ventricular wall with replacement of myo-

cardium by firm, white tissue; marked thinning of the apex resulted in apparent ventricular aneurysms. In transmural lesions, the adjacent endocardium was often white, firm, thickened, and glistening, with a "porcelain" appearance (Figure 3). The mean lesion grades for the three groups of rats were: 0.7 for 10–17 days of allylamine consumption (incidence, 2/7); 1.3 for 21–28 days (incidence, 4/7); and 3.0 for 90–104 days (incidence, 6/6). These gross lesion grades and the incidence of lesions following chronic allylamine administration are consistent with the degree of myocardial scarring observed and graded microscopially in our previous study.[9]

Light- and electron-microscopic study of scarred areas revealed predominantly dense mature collagen with scattered fibroblasts and capillaries. Occasional areas of scar were highly cellular; the cells in these areas contained irregularly shaped nuclei, prominent rough-surfaced endoplasmic reticulum, rare mitochondria, peripheral dense bodies similar to those seen in smooth-muscle cells,[12] bundles of thin filaments, prominent microtubules, and markedly irregular cell borders (Figures 4–6).

The intercellular matrix of these cellular areas was composed of mature collagen and occasional microfibrils associated with dense amorphous material consistent with elastin (Figures 5 and 7). Special staining of this material both in light- and electron-microscopic[11] preparations confirmed its identity as elastin (Figure 8).

Within areas of dense scar, occasional cardiac myocytes were completely surrounded by dense collagen. These myocytes were extemely degenerated, with markedly disoriented sarcomeres, distorted and condensed mitochondria, and fragments of intracellular desmosomes; intra- and extracellular spherical microparticles[13] were also present (Figures 9 and 10).

Small Vessel Alterations

Within and adjacent to scarred areas, small vessels with internal diameters of 15–30 μ displayed a promi-

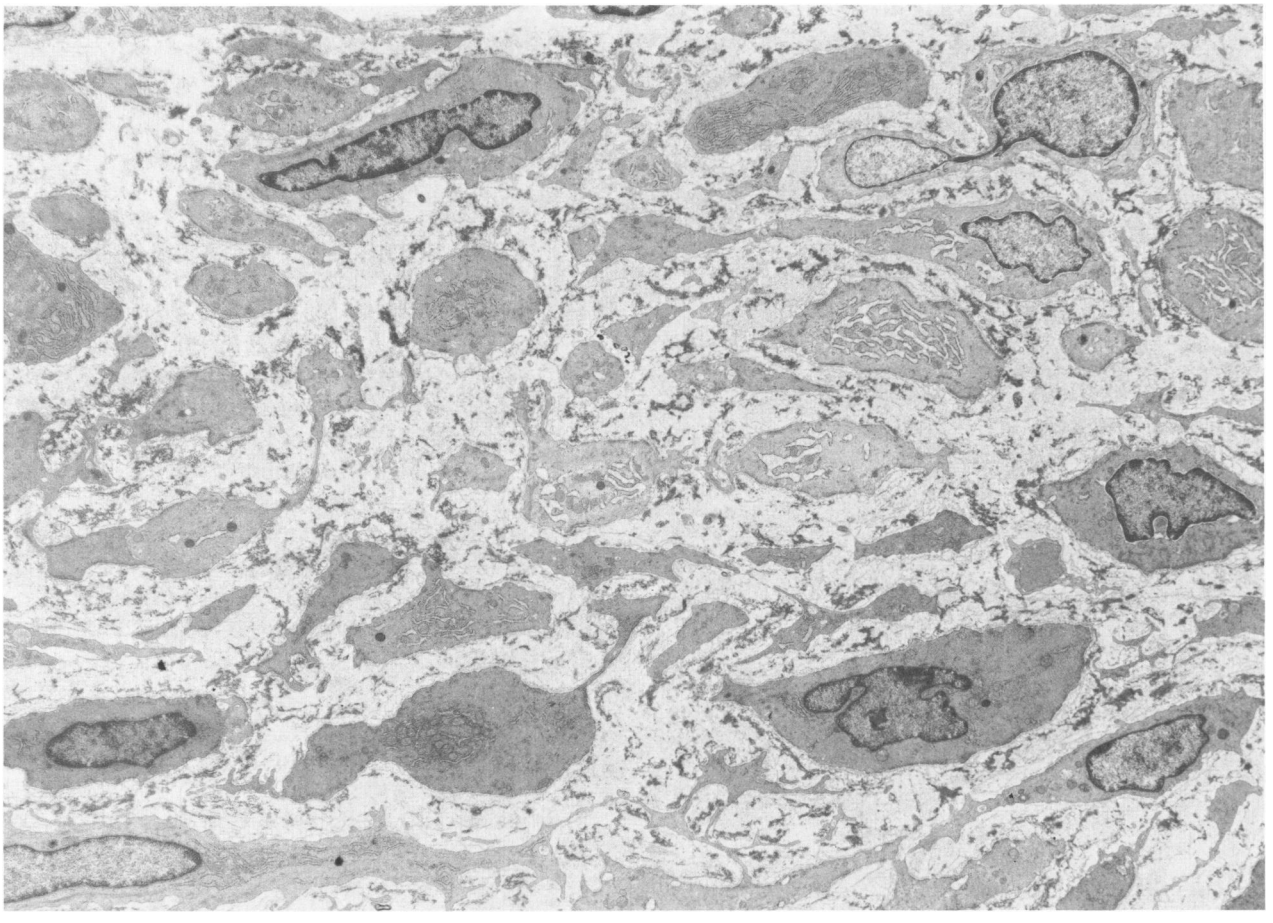

Figure 4—Low-power electron micrograph of a highly cellular area of scar containing numerous cells with irregularly shaped nuclei, irregular cell borders, abundant rough endoplasmic reticulum, and interstitium containing scattered patches of electron-dense elastin (see Figure 5). (×4400)

nent proliferation of cells between the vascular internal elastic lamina and the endothelial cells (Figure 11). The proliferating cells were smooth-muscle cells, as evidenced by peripheral dense bodies and prominent bundles of actinlike microfilaments. Endothelial cells remained intact, and no evidence of small-vessel thrombi was noted. Capillaries, small veins, and venules showed no lesions.

Endocardial Metaplasia

In areas of transmural fibrosis, focal endocardial cartilaginous and osseous metaplasia was found in two of the 6 animals receiving allylamine for 90–104 days (Figure 12). The metaplastic tissue was located near the endocardial surface, in strands of tissue which probably represented trabeculae carneae cordis of the left ventricle. Metaplasia was most frequently found in the left-ventricular endocardium but was also found in the right-ventricular endocardium.

The metaplastic cartilaginous areas were highly cellular. The chondrocytes in these areas (Figure 13) had uniform, oval or round nuclei and abundant rough endoplasmic reticulum and free ribosomes and were surrounded by lacunae containing microfibrils averaging 80 Å in diameter and scattered spicules that probably represented proteoglycan material. The intercellular matrix between chondrocytes consisted predominantly of dense collagen and scattered proteoglycan spicules. These features are ultrastructurally characteristic of fibrocartilage, rather than true hyaline cartilage.[14] In many areas, the collagen fibers within the matrix were undergoing calcification with a cross-banded pattern characteristic of calcifying connective tissue (Figures 14–16).

Areas of osseous metaplasia were characterized by osteocytes (Figure 17) which were morphologically similar to the chondrocytes but were located in lacunae surrounded by circular lamellae of densely calcified bone matrix. Canaliculi extended radially from the lacu-

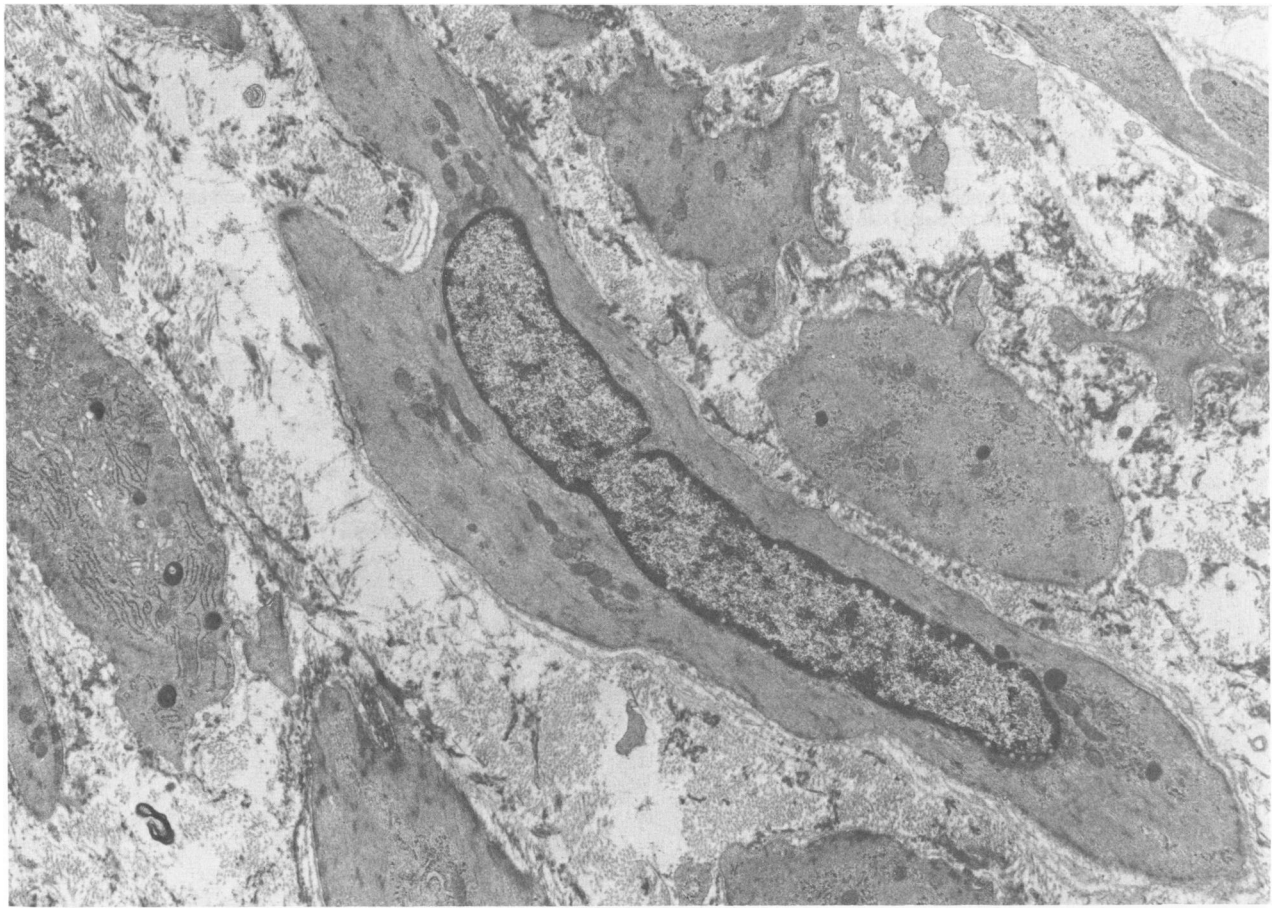

Figure 5—A cell within dense myocardial scar shows many characteristics of a smooth-muscle cell (myofibroblast), including an irregularly shaped nucleus, rare mitochondria, and peripheral dense bodies. The interstitium is composed of collagen and irregular patches of elastin. (×15,000)

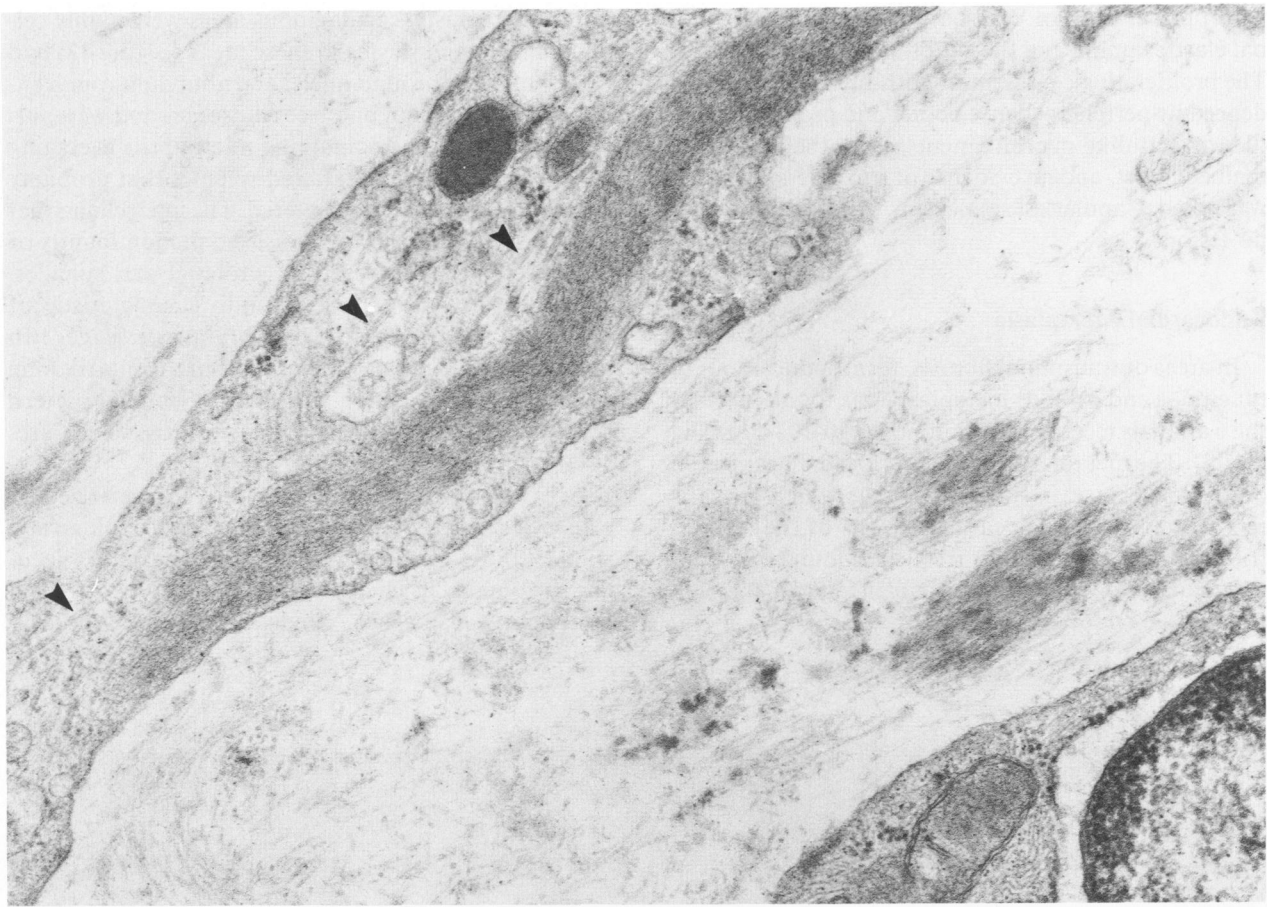

Figure 6—Higher-power view of cytoplasmic process of smooth-muscle-like cell embedded in scar consisting of collagen and elastin; note the bundle of thin filaments and microtubules (*arrows*). (×45,540)

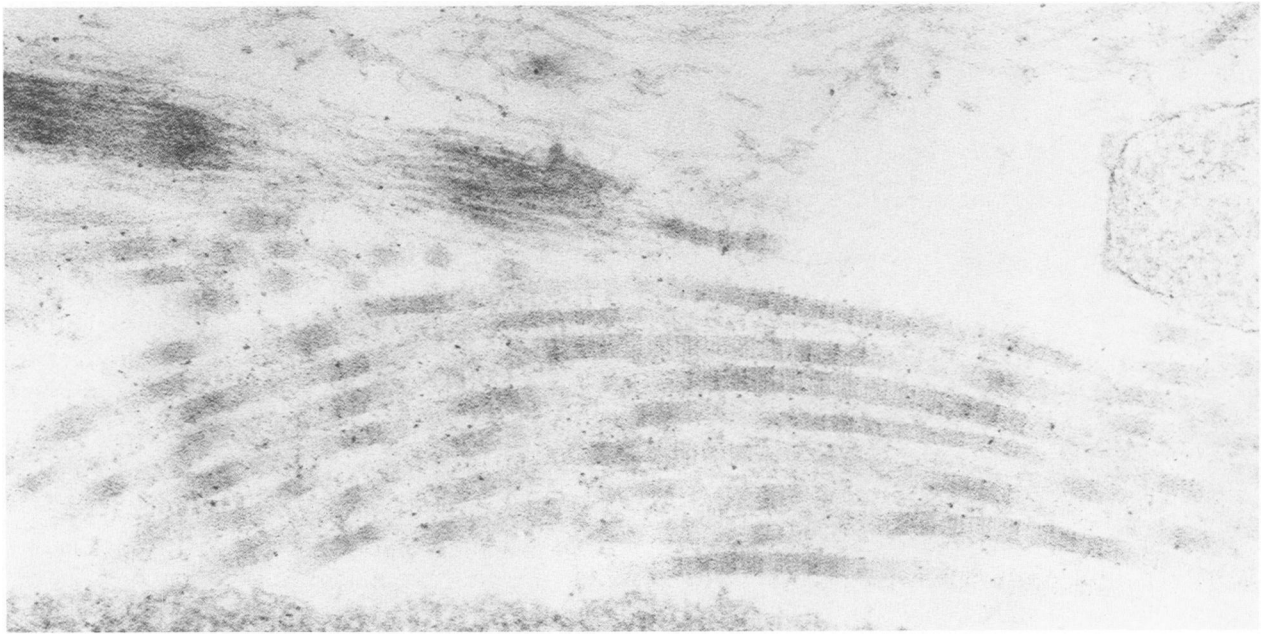

Figure 7—High-power view of interstitium within myocardial scar shows mature collagen with characteristic cross-banded pattern and microfibrils with dense amorphous material consistent with elastin. (×45,540)

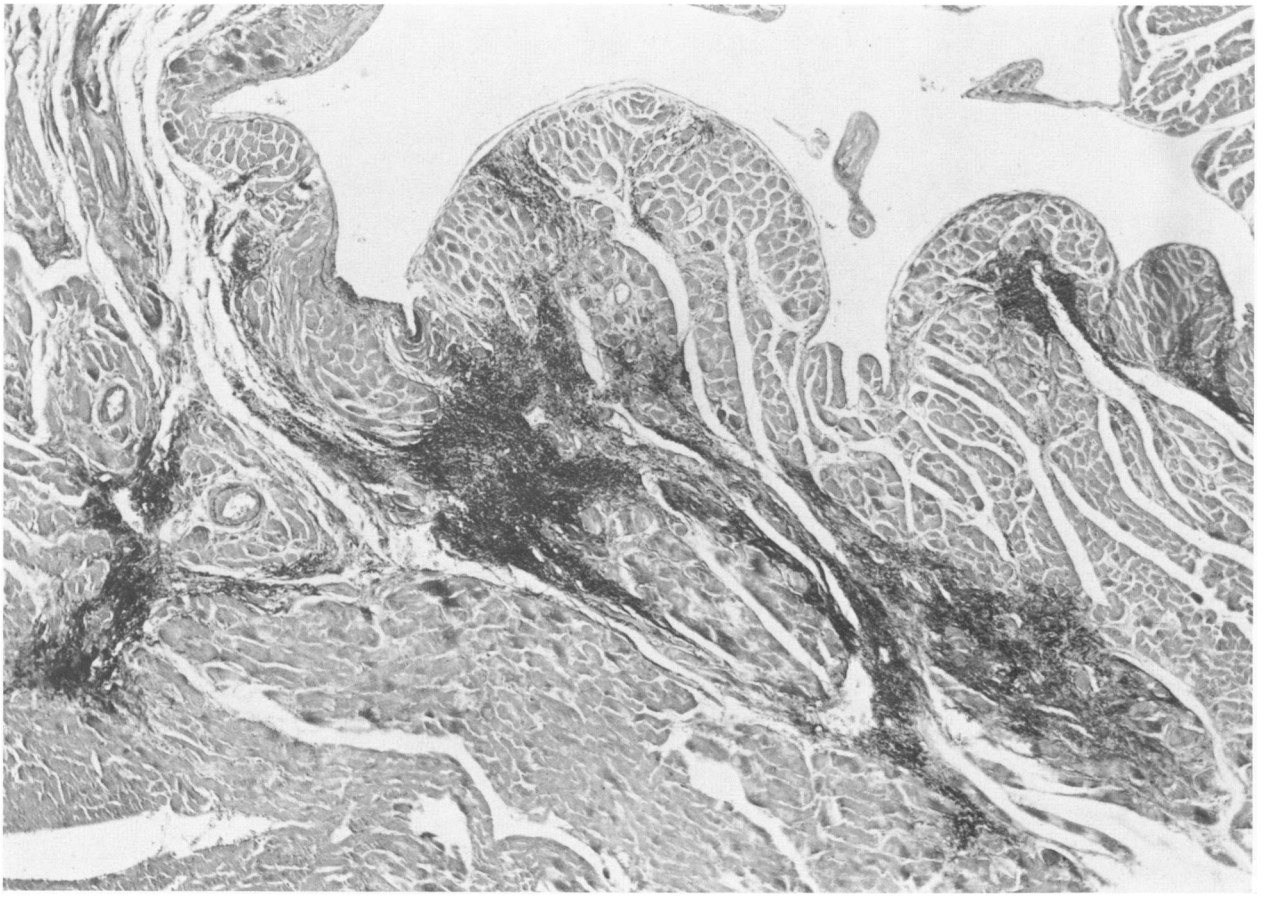

Figure 8—Light micrograph of left-ventricular subendocardial scar shows dark-staining irregular elastic fibers diffusely scattered throughout fibrous tissue. (Formalin fixation and Verhoeff–van Gieson stain, ×200)

nae and long, thin cellular extensions of the osteocytes were occasionally seen within canaliculi.

Discussion

Allylamine consumption causes progressive acute myocardial necrosis of areas which may vary in size from focal, individual cells to broader groups of myocytes. Therefore, at the earlier times examined in the present study (10–21 days), the major morphologic findings reflect organization of necrotic areas, predominantly in the subendocardium of the left ventricle. The progression of allylamine-induced myocardial injury results in extensive scarring which may resemble that seen in human left vetricular aneurysms.[2,3,9,10]

Microscopic scarring begins early in the course of allylamine-induced cardiac damage; in our previous study[9] we noted focal fibroblastic activity and fibrous tissue formation as early as 6 days after the start of allylamine consumption. By 21 days of consumption, the majority of rats in the present study showed grossly evident myocardial scarring. More prolonged consumption results in cumulatively greater scarring, as evidenced by progression of severity over a 36-day period in a previous study,[9] and by the continued occurrence of focal areas of myocardial necrosis and proliferation of fibroblasts throughout the entire period of consumption in the present study. The most noteworthy ultrastructural aspects of chronic allylamine-induced cardiac injury include 1) the extremely proliferative and fibroelastic nature of the mural scar; 2) the intimal proliferation of smooth-muscle cells in small myocardial arteries, and 3) the bizarre cartilaginous and osseous metaplasia observed in endocardium.

Nature of the Mural Scar

The major component of the scars observed in this study was dense, mature collagen. Focal areas of extensive elastin formation were also present. The proliferating cells observed within scars appeared to have many characteristics of both smooth-muscle cells and fibro-

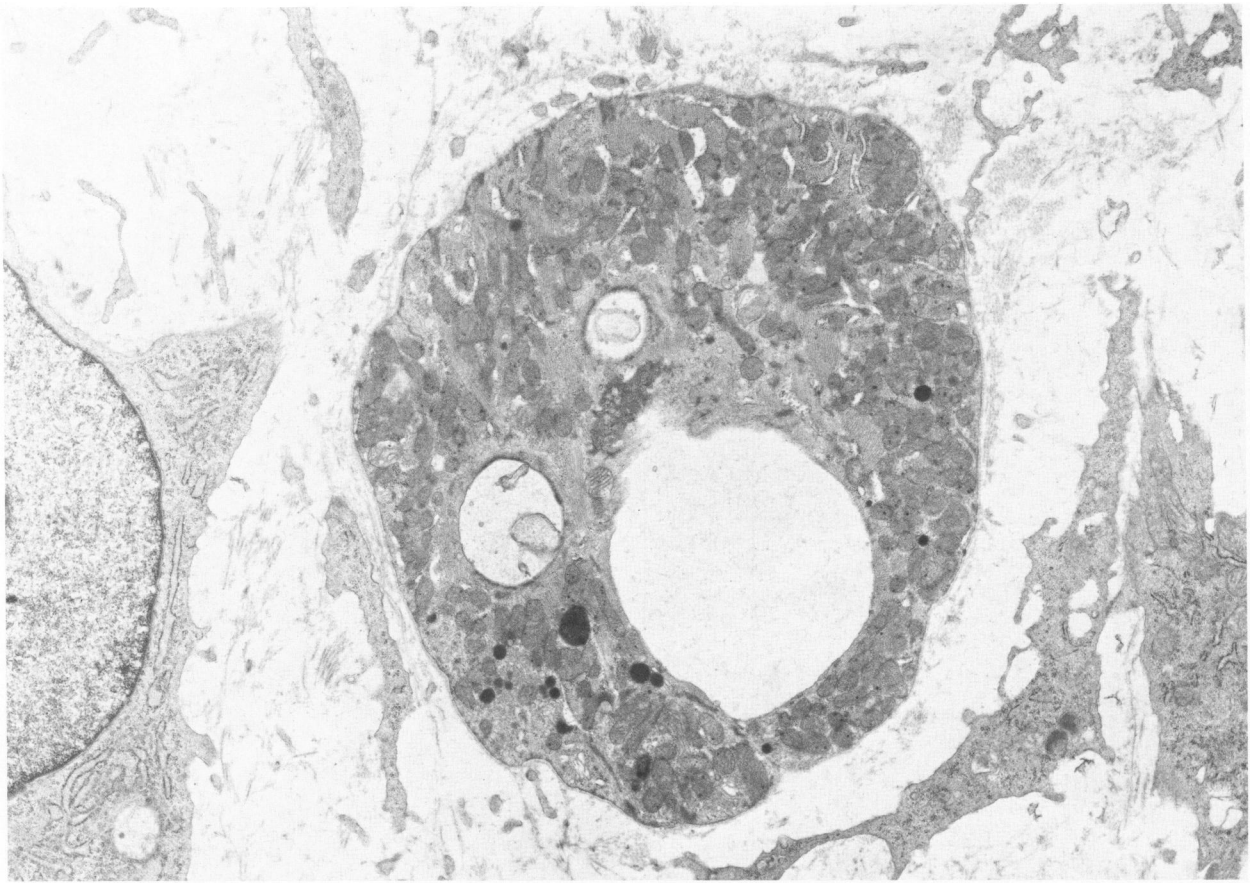

Figure 9—A markedly degenerated myocyte embedded in dense myocardial scar shows extremely deranged sarcomeres, and distorted, condensed mitochondria (see Figure 10). (×9580)

blasts, and therefore may be considered myofibroblasts.[15] These cells contain bundles of packed myofilaments resembling those found in smooth muscle.[12] These filaments may be related to a contractile function found in wound granulation tissue,[15-19] in the nodules of fibrous tissue involving the palmar aponeurosis in Dupuytren's contracture,[20] in the fibrous reaction to silicone prostheses,[21,22] and in the arterial media of human dysplastic renal arteries.[23] Cells in these diverse fibrotic conditions, and those found in the myocardial scars in the present study, also have convoluted nuclei with many folds and indentations, subsarcolemmal electron-dense areas which are characteristic of smooth-muscle cells,[19] microtubules,[24] and extracellular basement membrane material near the sarcolemma. A similar morphologic spectrum of cells, varying from fibroblasts to myofibroblasts and smooth-muscle cells, also has been described in the thickened endocardium found in human endocardial fibroelastosis.[25,26]

In our study, myofibroblasts were found in areas of collagen and elastin production, and the presence of scattered rough endoplasmic reticulum within these cells suggests that they are actively synthesizing the surrounding matrix. Smooth-muscle cells have been shown to produce both collagen and elastin in culture,[27,28] and although most reports concerning myofibroblasts do not associate them with elastin, it seems reasonable to assume that they are capable of elastin production.[15]

Another finding of this study is the gross (Figure 3) and microscopic similarity to endocardial fibroelastosis exhibited by the severely scarred hearts of allylamine-treated rats. Endocardial fibroelastosis occurs in a primary form[29,30] and in a secondary form which may be associated with a variety of congenital cardiac anomalies (see Schryer and Karnauchow[31] for a review). Endocardial fibroelastosis also can be secondary to a variety of pathologic processes which result in endomyocardial injury, including ischemic injury.[29,32]

Morphologically, both forms of endocardial fibroelastosis are characterized by diffuse thickening of the left ventricular endocardium by firm white tissue. In the primary form the elastic fibers are thick and large

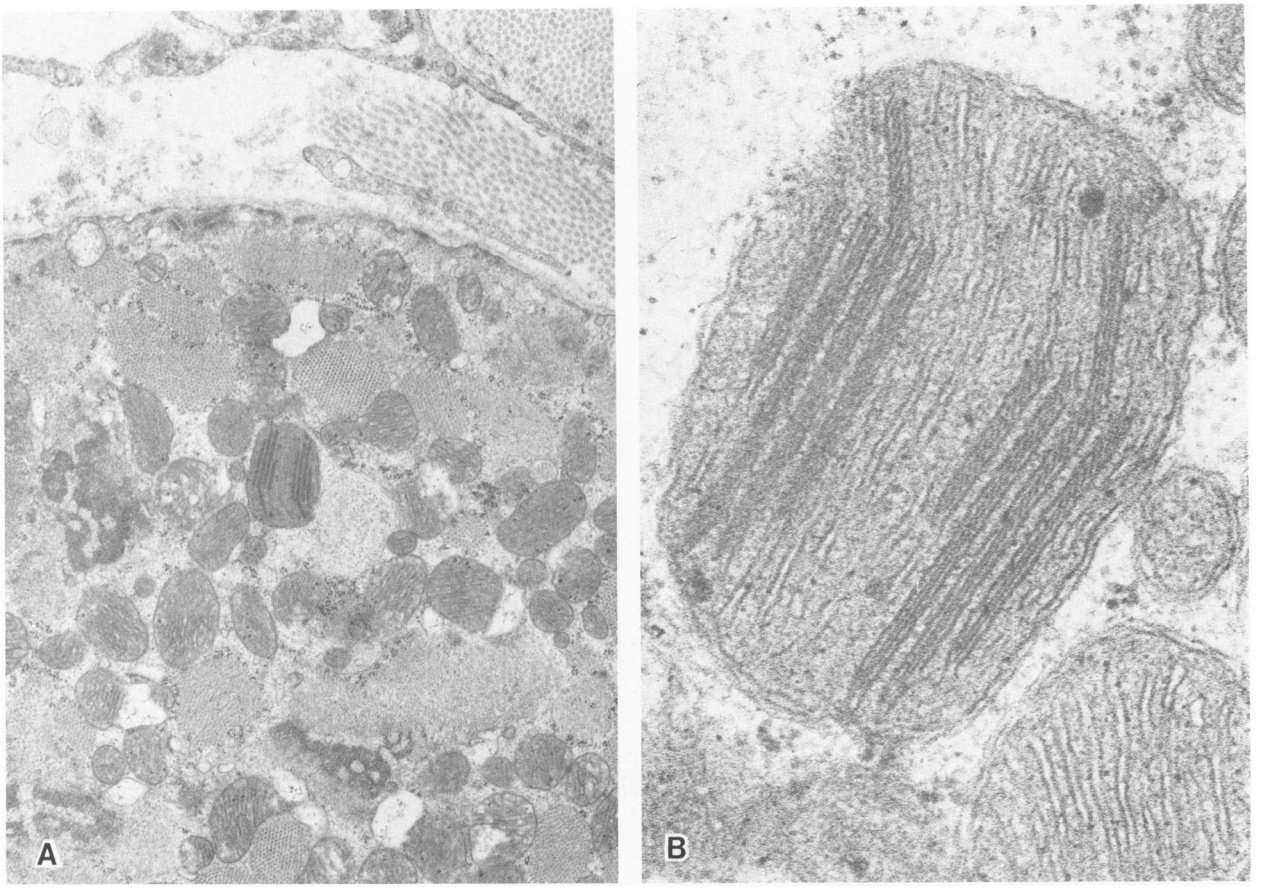

Figure 10A—A markedly degenerated myocyte shows markedly abnormal, condensed mitochondria of variable size and shape. (×12,000) **B**—High-power view of the abnormal mitochondrion seen in **A** shows cristae condensed into platelike membranous structures with a spiraling arrangement. (×75,000)

(1–2 μ in diameter), while in the secondary form they are smaller and less well oriented.[27] The small, irregularly arranged elastic fibers in the transmural scars induced by allylamine consumption (see Figures 4 and 8) are similar to those in the secondary form of endocardial fibroelastosis.

Many causes have been postulated for the development of endocardial fibroelastosis,[29,30,33] but in allylamine cardiotoxicity it seems likely that elastic tissue formation is a reactive phenomenon occurring in severely damaged, scarred areas in response to abnormal wall tension, hypoxia, or to late toxic effects of the chemical itself or its metabolites.

Small Vessel Alterations

In this study, we observed proliferation of smooth-muscle cells within the intima of small myocardial arteries. These vessels, which varied from 10 to 30 μ, correspond to small terminal arterioles or precapillary sphincters.[34] Previous studies of allylamine intoxication have described similar proliferative lesions in the larger coronary arteries[5–8] and also other systemic arteries[35] of the rat. Although other authors have suggested that these obstructive lesions may cause ischemia and, hence, may result in allylamine-induced myocardial necrosis, our previous light-microscopic studies[9,10] have shown that arterial lesions do not begin to occur until 21 days of allylamine consumption, when cardiac necrosis and scarring are already well established.

Obstructive small vessel lesions which are morphologically similar to those described in this study have been shown to occur in humans with hypertrophic cardiomyopathy,[36] scleroderma,[37] Friedreich's ataxia,[38,39] juvenile diabetes mellitus,[40] and in the cardiomyopathy of adult Africans in Rhodesia.[41] Morphologically similar proliferations of smooth-muscle cells have been experimentally induced in larger arteries by a variety of traumatic techniques[42–44]; such lesions also occur spontaneously in the chicken[45] and steelhead trout.[46] Few, if any, ultrastructural studies have been made of smooth-muscle cell proliferation in these pathologic sit-

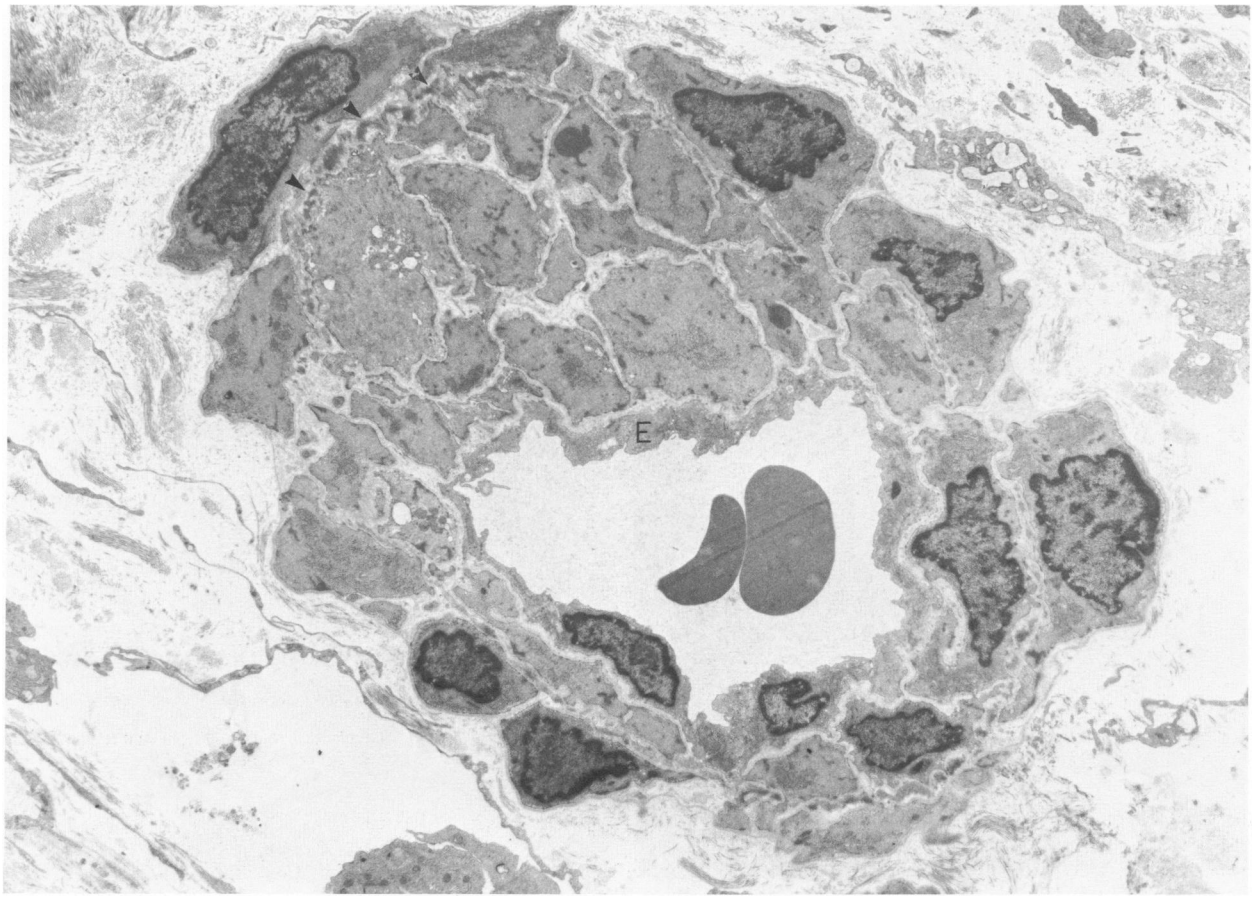

Figure 11—A small vessel within myocardial scar shows smooth-muscle cell proliferation between the endothelial cell (*E*) and the internal elastic lamina (*arrows*). (×3800)

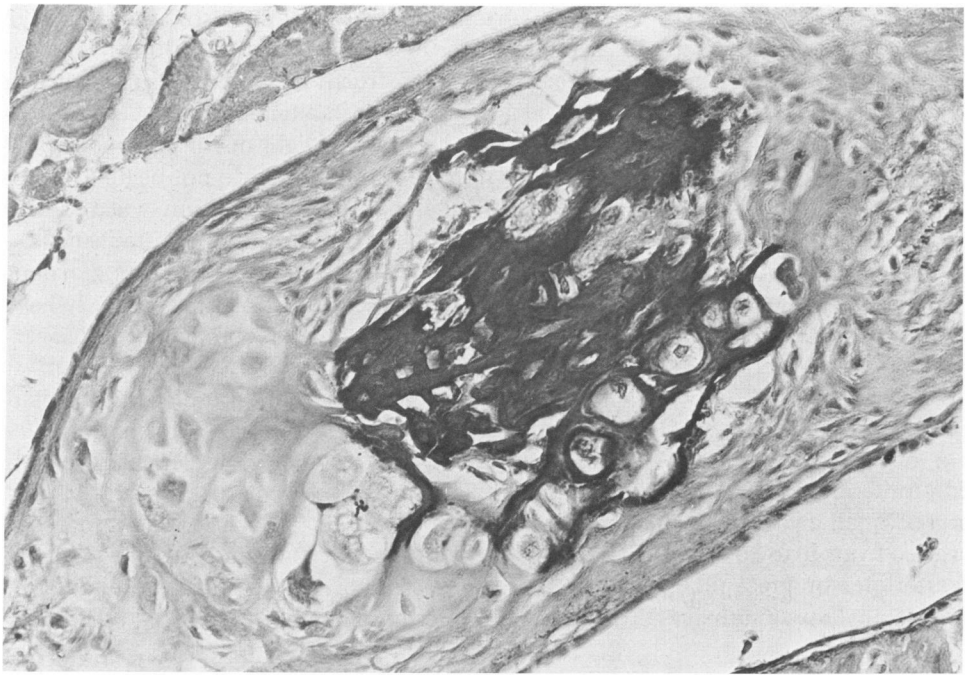

Figure 12—Light micrograph of metaplastic tissue found in the subendocardial area of transmural ventricular scar shows cartilage with the light-microscopic appearance of cartilage (*left*, see Figure 13) and darkly stained calcified bone (*right*, see Figure 17). (Formalin fixation; Masson's trichrome, ×731)

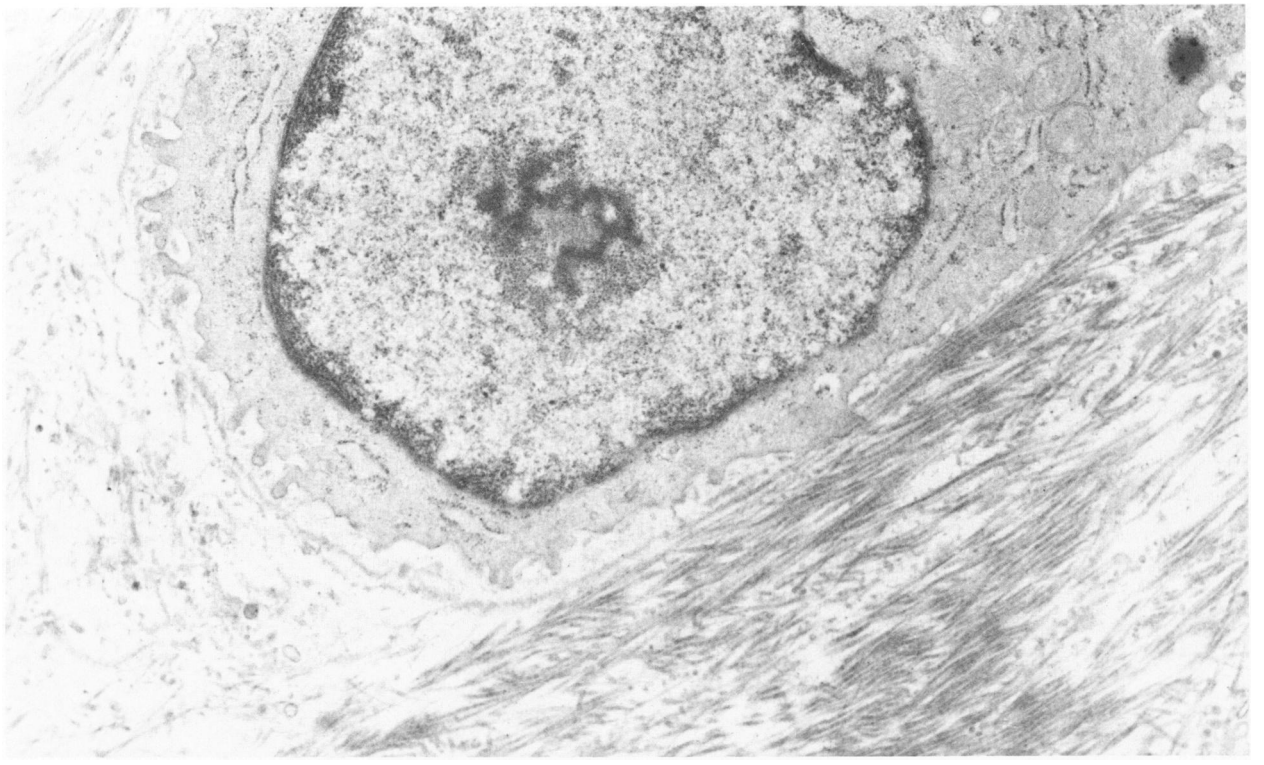

Figure 13—Cartilage cell within an area of metaplastic tissue shows a uniform nucleus with a prominent nucleolus, rough endoplasmic reticulum, and few mitochondria. The surrounding pericellular space contains cartilage matrix and dense intercellular collagenous fibrils. (×14,900)

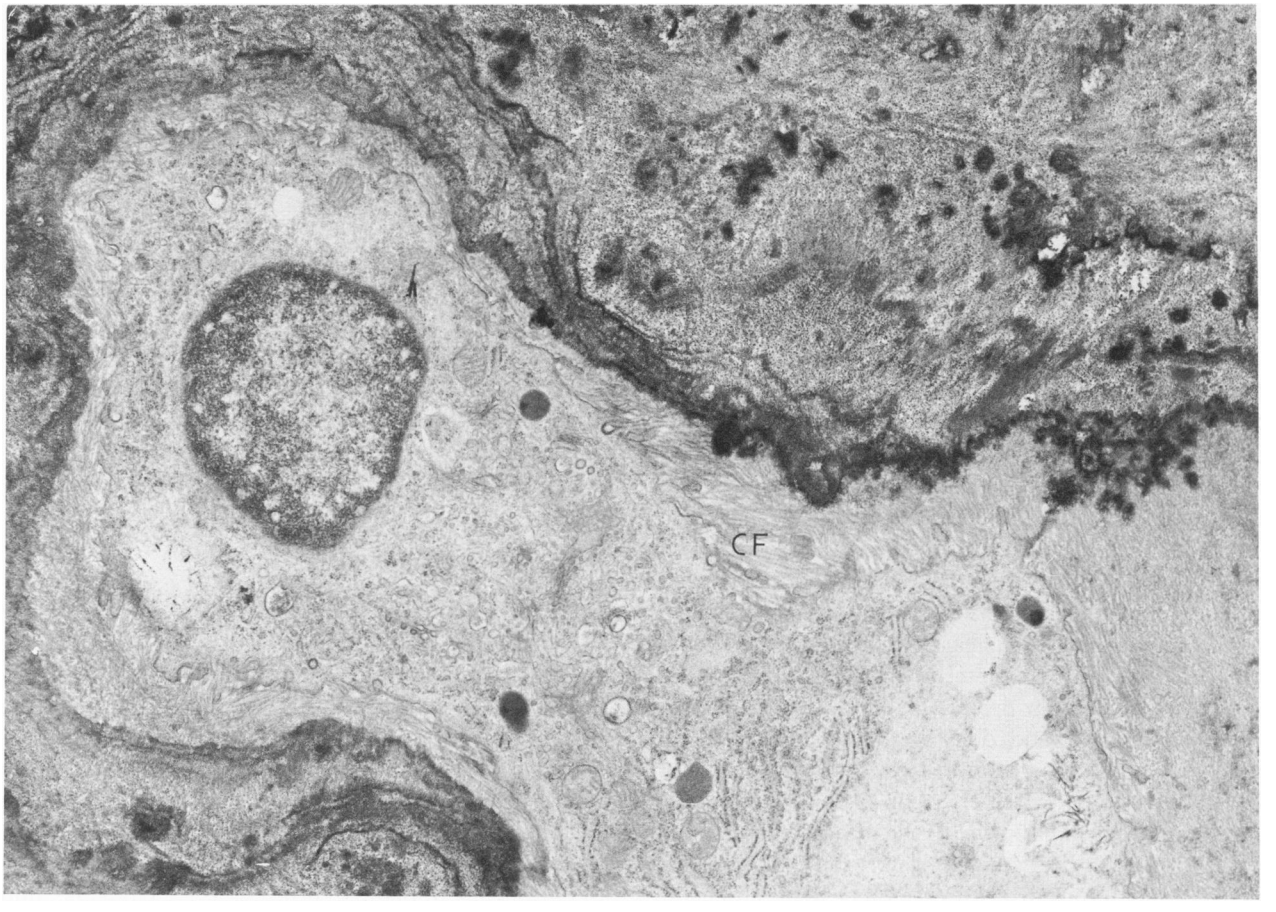

Figure 14—Within an area of calcifying metaplastic tissue, a cartilagelike cell is surrounded by collagen fibrils (*CF*), which are undergoing calcification evidenced by irregular, dark, concentric lines around the cell. (×10,500)

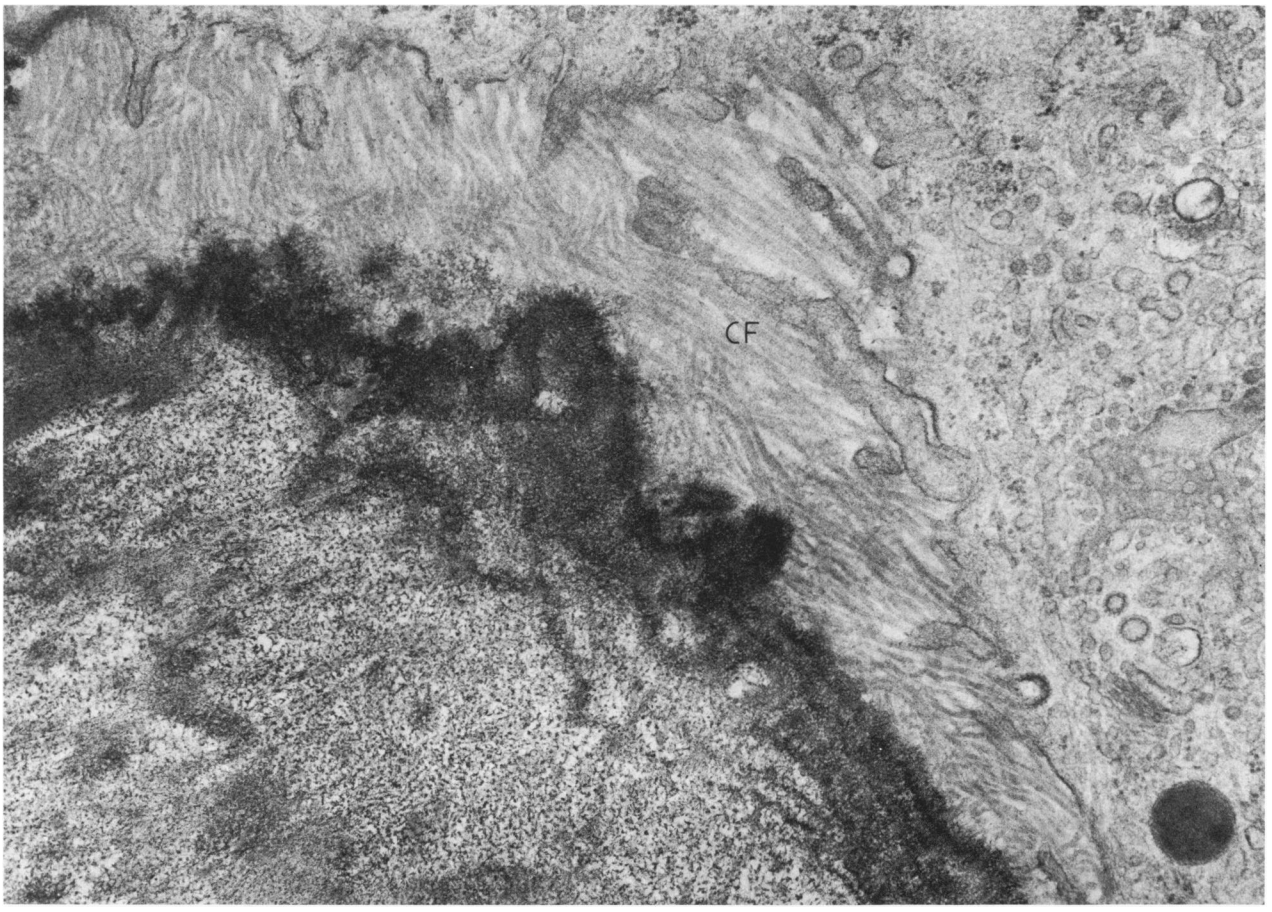

Figure 15—A high-power of view of calcifying metaplastic tissue as shown in Figure 14 demonstrates the cytoplasm of the cartilagelike cell (*above, right*), the collagen fibrils (*CF*), line of dense calcification, and diffuse spicules of calcium salts. (×31,500)

uations, and the reasons for intimal smooth-muscle proliferation in those diverse experimental and natural situations are unknown.

Allylamine has been known to be a potent vascular toxin for many years, and a variety of investigators have used its toxicity to study vascular injury. Mellon et al,[47] in 1935, concluded that allylamine given intradermally caused a necrotizing arteriolitis which was independent of pH and seemed to initially affect the vascular wall. Their photomicrographs show extensive medial necrosis. Subsequent histochemical and biochemical studies of aortic and coronary arterial wall have demonstrated an allylamine-induced increase in glycogen,[48,49] accumulation of PAS-positive material presumed to be heterogeneous polysaccharides,[49] and alterations in phosphomonoesterase and dehydrogenase enzymes.[50] In addition, allylamine administered intravenously has been shown to be extremely toxic to endothelial cells, presumably causing rupture of the plasmalemma.[51] Recent *in vitro* studies[52,53] have shown that allylamine is actively metabolized to an extremely toxic aldehyde, acrolein, by cardiovascular tissues, especially by aorta and coronary arteries. Although the cellular localization of this metabolic process is unknown, we suspect that vascular smooth muscle may be involved. It seems reasonable to hypothesize that the toxin itself or its metabolite—acrolein—may have a toxic, stimulatory effect on smooth-muscle cells, resulting in the proliferation of these cells in certain vessels.

Endocardial Metaplasia

Hyaline cartilage occurs normally in the aortic ring in mammals and reptiles.[54–56] Aortic and mitral valve structures may undergo cartilaginous and bony metaplasia following degeneration secondary to chronic endocarditis with valvular aneurysm in the dog[57] or severe valvular stenosis with calcification and deposition of atherosclerotic material in the human,[58] as has been the personal observation of the author, Paul J. Boor. Metaplastic cartilage also occurs in the heart at sites of chronically implanted intravenous pacemakers[59] and

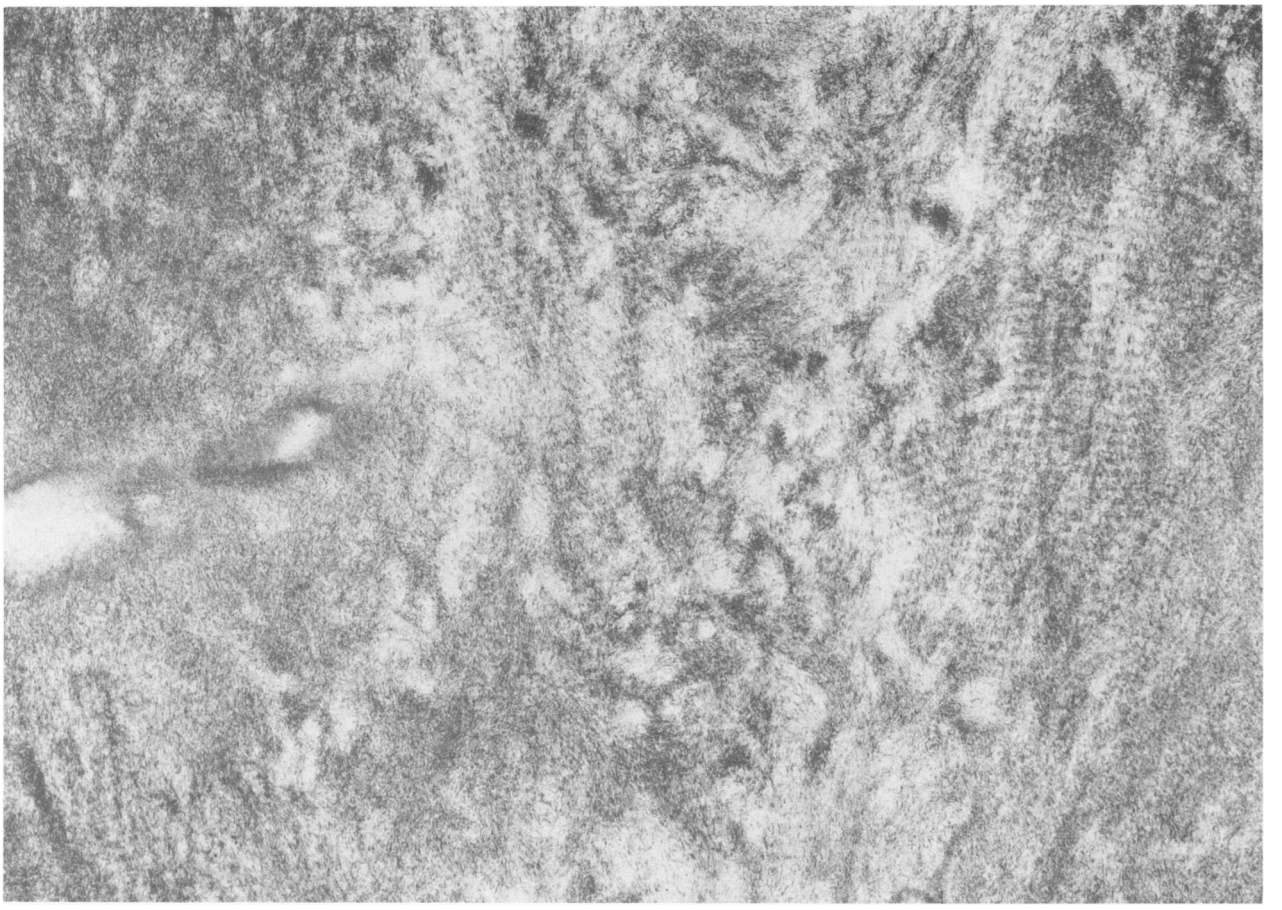

Figure 16—A high-power view of calcifying metaplastic tissue shows a cross-banded pattern with periodicity (~640 Å) characteristic of calcifying collagenous matrix. (×60,000)

automatic defibrillator leads,[60,61] in organizing atrial thrombi in the syndrome of arterial thrombosis in aging rodents,[62] and in the thickened endocardium of cats with restrictive cardiomyopathy.[63]

The metaplastic tissue which we observed beginning in rats after 21 days of allylamine consumption had the ultrastructural appearance of fibrocartilage, calcifying cartilage and connective tissue, and mature bone.[14] These metaplastic tissues were always found in endocardial trabeculae carneae near areas of extensive transmural myocardial scarring or ventricular aneurysms. It is unlikely that the cartilage observed actually formed in organized mural thrombi, because thrombi in this location were very rarely found in our previous study.[10]

The lesions in our model of allylamine-induced myocardial necrosis bear many similarities to the isoproterenol-induced lesions described by Rona and Kahn,[64] including not only the endocardial metaplasia, but also the inflammatory component of the necrosis and the exuberant proliferation in the scar. Rona and Kahn observed dense scar formation beginning at 8–12 weeks after isoproterenol administration but noted cartilaginous and bony metaplasia in the walls of ventricular aneurysms only after very prolonged periods (16 and 32 weeks). The metaplastic tissue observed in their study was apparently localized in endocardial structures—as was that described in our study—and they considered the metaplastic bony lamellae to be growing parallel to the endocardial surface.

Bone and cartilage have been induced experimentally in a variety of extraosseous sites by the implantation of devitalized tissues,[65] extracts of bone,[66] and formaldehyde injection.[59] Experimental aortic injury due to grafts or sutures results in cartilaginous metaplasia.[67] Rodbard suggested that abnormal mechanical properties, such as increased stiffness, resulted in aortic chondroid metaplasia[68]; still other workers have hypothesized a soluble chondrogenic factor.[69] McCandless and co-workers[70] induced cartilage formation in chicken aorta and myocardium by injections of the sulfated polysaccharide, carrageenan. Metaplastic changes have not been noted in experimental models of cardiac isch-

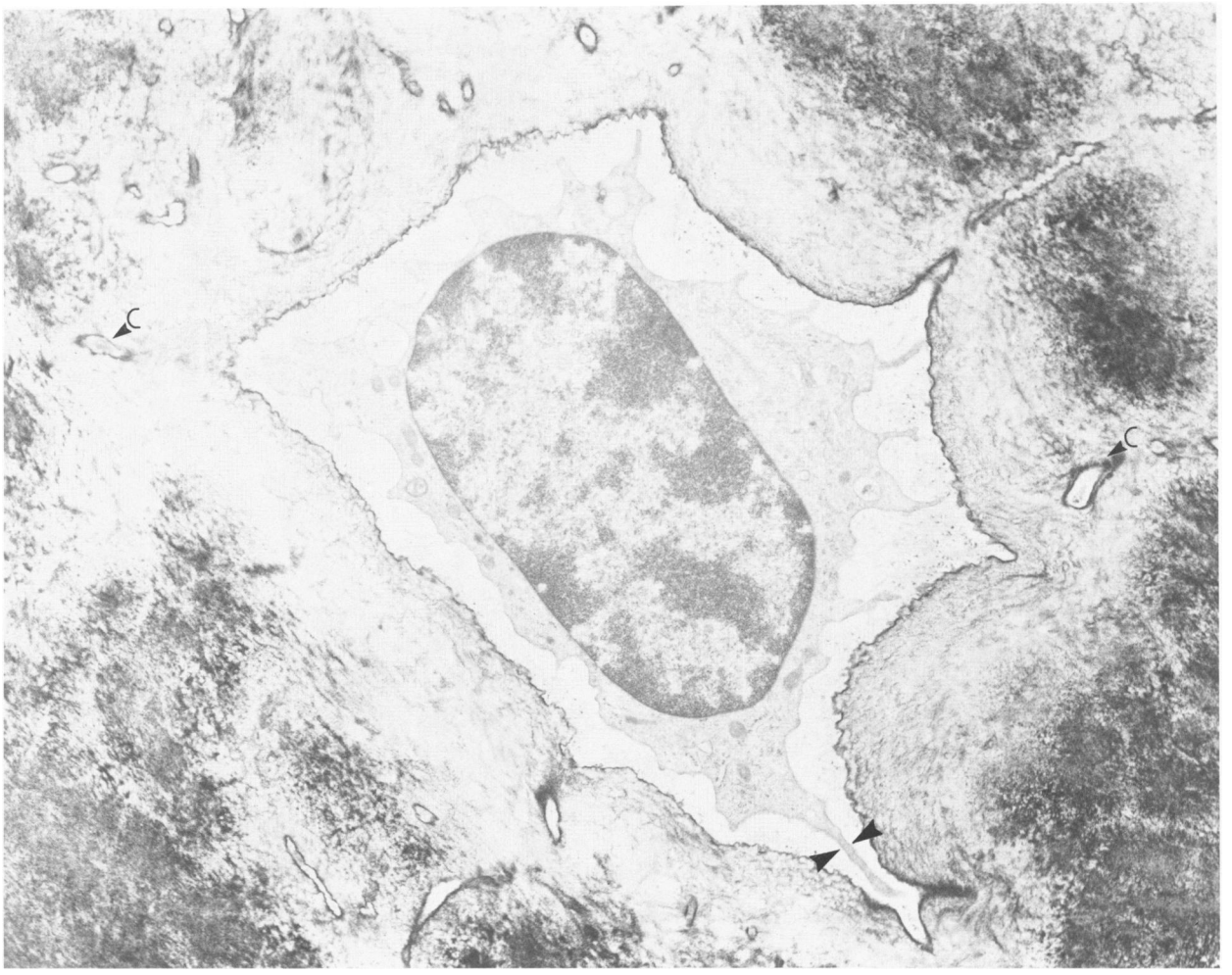

Figure 17—Within subendocardial metaplastic tissue, a mature osteocyte is surrounded by a lacunar space and dense, calcified bone matrix. Note numerous canaliculi (*C*) and a cytoplasmic process (*arrowheads*) extending toward a canaliculus. (×13,800)

emia[49,64,71]; however, Lehoczky-Mona and McCandless[72] found that prior coronary ligation increased the incidence of carrageenan-induced cartilage in myocardium, suggesting that tissue hypoxia can modulate myocardial chondrogenesis.

The concept that tissue ischemia or hypoxia favors cartilaginous or bony metaplasia is supported by recent studies of the initiating factors of tissue calcification in the epiphyseal growth plate. As proliferating chondrocytes begin to form calcified matrix along the normal growth plate, they release cellular calcium and phosphate ions.[73,74] The source of these ions is believed to be the chondrocyte mitochondria,[75] which have concentrated ions in the premineralized area of chondrocytes, and the stimulus for ion release is hypothesized to be low oxygen tension in the tissue[76] and a shift in the NADH/NAD^+ ratio to the reduced state.[77] Hence, localized anoxia and the consequent shift in tissue redox state may also favor formation of calcified cartilage and bone in certain damaged, anoxic soft tissues such as aorta. In fact, the concept that bone and cartilage formation is favored in areas of anoxia and poor vascular flow dates back to 1930, when Ham, in his study of fracture repair,[78] concluded that cartilage formation was favored in areas of ischemia.

No clear explanation is evident for the endocardial metaplasia that we have observed in allylamine-induced cardiomyopathy in the present study. It seems likely that an unknown combination of metabolic factors may result in the propensity of the endocardium to undergo metaplasia in this experimental model of allylamine-induced cardiomyopathy, as well as in the cardiac injury caused by large doses of isoproterenol.[64]

In conclusion, the ultrastructural features of chronic allylamine-induced cardiac lesions include 1) a dense collagenous scar with many active myofibroblasts, 2) areas of elastin formation with features resembling those in the secondary form of endocardial fibroelasto-

sis, 3) intimal proliferation of smooth-muscle cells in small intramyocardial arterioles and arteries, and 4) bizarre endocardial cartilaginous and bony metaplasia. Although there is no one unifying cause which can explain this variety of lesions, they clearly indicate severe chronic myocardial and endocardial injury during the course of long-term allylamine intoxication.

References

1. Boor PJ, Ferrans VJ: Ultrastructural alterations in allylamine induced cardiomyopathy: Early lesions. Lab Invest 1982, 47:76–86
2. Lalich JJ, Paik WCW: Influence of hydralazine consumption in allylamine-induced myocardial fibrosis and hypertrophy in rats. Exp Mol Pathol 1974, 21:29–39
3. Lalich JJ: Coronary artery hyalinosis in rats fed allylamine. Exp Mol Pathol 1969, 10:14–26
4. Paik WCW, Lalich JJ: Factors which contribute to aortic fibrous repair in rats fed β-aminopropionitrile. Lab Invest 1970, 22:28–35
5. Inouye DK: Vascular lesions in Rhesus monkeys fed allylamine. Fed Proc 1971, 30:293
6. Waters LL: Changes in the coronary arteries of the dog following injections of allylamine. Am Heart J 1948, 35:212–220
7. Bloor CM, Lowman RM: Experimental coronary arteriography: The distribution and extent of allylamine-induced vascular lesions in the dog. Radiology 1963, 81:770–789
8. Lalich JJ, Allen JR, Paik WCW: Myocardial fibrosis and smooth muscle cell hyperplasia in coronary arteries of allylamine-fed rats. Am J Pathol 1972, 66:225–240
9. Boor PJ, Moslen MT, Reynolds ES: Allylamine cardiotoxicity: I. Sequence of pathologic events. Toxicol Appl Pharmacol 1979, 50:581
10. Boor PJ, Nelson TJ, Chieco P: Allylamine cardiotoxicity: II. Histopathology and histochemistry. Am J Pathol 1980, 100:739
11. Kajikawa K, Yamaguchi T, Katsuda S, Miwa A: An improved stain for elastic fibers using tannic acid. J Electron Microsc (Tokyo) 1975, 24:287
12. Rhodin, JAA: Fine structure of vascular walls in mammals. Physiol Rev 1962, 42:48–81
13. Ferrans VJ, Thiedemann K-U, Maron BJ, Jones M, Roberts WC: Spherical microparticles in human myocardium: an ultrastructural study. Lab Invest 1976, 35: 349–368
14. Rhodin JAG, Histology. New York, Oxford University Press, 1974 pp 173–202
15. Gabbiani G, Ryan GB, Majno G: Presence of modified fibroblasts in granulation tissue and their possible role in wound contraction. Experientia 1971, 27:549–550
16. Ryan GB, Cliff WJ, Gabbiani G, Irle C, Montandon D, Srarkov PR, Majno G: Myofibroblasts in human granulation tissue. Hum Pathol 1974, 5:55–67
17. Gabbiani G, Chaponnier C, Huttner I: Cytoplasmic filaments and gap junctions in epithelial cells and myofibroblasts during wound healing. J Cell Biol 1978, 76:561–568
18. Baur PS, Larson DL, Stacey TR: The observation of myofibroblasts in hypertrophic scars. Surg Gynecol Obstet 1975, 141:22–26
19. Gabbiani G, Montandon D: Reparative processes in mammalian wound healing: The role of contractile phenomena. Int Rev Cytol 1977, 48:187–219
20. Gabbiani G, Majno G: Dupuytren's contracture: Fibroblast contraction? Am J Pathol 1972, 66:131–138
21. Chamay A, Gabbiani G: Digital contracture deformity after implantation of a silicone prosthesis: Light and electron microscopic study. J Hand Surg 1978, 3:266–270
22. Rudolph R, Abraham J, Vecchione T, Guber S. Woodward M: Myofibroblasts and free silicon around breast implants. Plast Reconstr Surg, 1978, 62:185–195
23. Sottiurai VS, Fry WJ, Stanley JC: Ultrastructure of medial smooth muscle and myofibroblasts in human arterial dysplasia. Arch Surg 1978, 113:1280–1288
24. Rudolph R, Woodward M: Spatial orientation of microtubules in contractile fibroblasts *in vivo.* Anat Rec 1978, 191:169–182
25. Sekiguchi M, Hirosawa K: Ultrastructural assessment of endocardial fibroelastosis using the endocardial biopsy technique. J Clin Electron Microsc 1973, 6:220–221
26. Neustein HB, Lurie PR, Fujita M: Endocardial fibroelastosis found in transvascular endomyocardial biopsy in children. Arch Pathol Lab Med 1979, 103:214–219
27. Mecham RP: Elastin biosynthesis: A look at the current scene. Connect Tissue Res 1981, 8:155–160
28. Sandberg LB, Leslie JG, Oakes BW: In vitro studies of elastin metabolism. Connect Tissue Res 1981, 8:219–225
29. Fishbein MC, Ferrans VJ, Roberts WC: Histologic and ultrastructural features of primary and secondary endocardial fibroelastosis. Arch Pathol Lab Med 1977, 101:49–54
30. Paasch LH, Zook BC: The pathogenesis of endocardial fibroelastosis in burmese cats. Lab Invest 1980, 42:197–204
31. Schryer MJP, Karnauchow PN: Endocardial fibroelastosis: Etiologic and pathogenetic considerations in children. Am Heart J 1974, 88:557–565
32. Roberts WC, Bulkley BH, Morrow AG: Pathologic anatomy of cardiac valve replacement: A study of 224 necropsy patients. Prog Cardiovasc Dis 1973, 15:539–587
33. Hutchins GM, Vie SA: The progression of interstitial myocarditis to idiopathic endocardial fibroelastosis. Am J Pathol 1972, 66:483–496
34. Rhodin JAG: The ultrastructure of mammalian arterioles and precapillary sphincters. J Ultrastruct Res 1967, 18:181–223
35. Simpson CF: Coronary and thyroid arteriopathy induced by allylamine and β-amino propionitrile. Exp Molec Pathol 1982, 37:382–392
36. James TN, Marshall TK: Asymmetrical hypertrophy of the heart. Circulation 1975, 51:1149–1166
37. James TN: Coronary arteries and conduction system in scleroderma heart disease. Circulation 1974, 50:844–856
38. James TN, Fisch C: Observation on the cardiovascular involvement in Friedreich's ataxia. Am Heart J 1963, 66:164–175
39. Nadas AS, Alimurung MM, Sieracki LA: Cardiac manifestations of Friedreich's ataxia. N Engl J Med 1951, 244:239–244
40. James TN: Small arteries of the heart. Circulation 1977, 56:2–14
41. Johns INP, Olson BJ: Experimental myocardial infarction: I. A method of coronary occlusion in small animals. Ann Surg 1954, 140:675–682
42. Guyton JR, Karnovsky MJ: Smooth muscle cell proliferation in the occluded rat carotid artery. Am J Pathol 1979, 94:585–602
43. Imparato AM, Baumann FG, Pearson J, Kim GE, Davidson T, Ibrahim I, Nathan I: Electron microscopic studies of experimentally produced fibromuscular arterial lesions. Surg Gynecol Obstet 1974, 139:497–504
44. Thomas WA, Kim DN: Atherosclerosis as a hyperplastic and/or neoplastic process. Lab Invest 1983, 48:245–255
45. Moss NS, Benditt EP: The ultrastructure of spontaneous and experimentally induced arterial lesions: II. The spontaneous plaque in the chicken. Lab Invest 1970, 23:241–245
46. House EW, Benditt EP: The ultrastructure of spontane-

ous coronary arterial lesions in steelhead trout. Am J Pathol 1981, 104:250–257
47. Mellon RR, Baker MR, McIhoy AP: Experimental necrotizing arteriolitis induced by a protein cleavage product. Proc Soc Exp Biol Med 1935, 33:192–195
48. Norcia LN, Gonzalez IE, Shetlar MR, Peter JA, Furman RH: Alterations of protein, lipid and polysaccharide composition of canine aortas induced by allylamine, gonadal steroids and castration. Am J Physiol 1958, 195:759–768
49. Conrad LL, Gonzalez IE, Joel W, Furman RH: Histochemical evaluation of canine coronary artery and aortic lesions induced by intravenous allylamine. Circ Res 1956, 4:263–267
50. Zemplenyi T, Mrhóva O, Urbanova D: Allylamine-induced arterial enzyme changes and the role of injury in atherogenesis. Circulation 1969, 40 (Suppl):27
51. Constantinides P, Robinson M: Ultrastructural injury of arterial endothelium: II. Effects of vasoactive amines. Arch Pathol 1969, 88:106–112
52. Boor PJ, Nelson TJ: Biotransformation of the cardiovascular toxin, allylamine, by rat and human cardiovascular tissue. J Mol Cell Cardiol 1983, 14:679–682
53. Nelson TJ, Boor PJ: Allylamine cardiotoxicity: IV. Metabolism to acrolein by cardiovascular tissues. Biochem Pharmacol 1982, 31:509–514
54. Hollander CF: Cartilaginous focus at the base of the noncoronary semilunar valve of the aorta in rats of different ages. Exp Gerontol 1968, 3:303–307
55. Kelsall MA, Visci M: Aortic cartilage in the heart of Syrian hamsters. Anat Rec 1970, 166:627
56. Hueper WC: Cartilaginous foci in the hearts of white rats and of mice. Arch Pathol 1939, 27:466–468
57. Spiegel A: Histologische Untersuchungen über Endokarditis beim Hunde nebst einem Anhang über einige seltenere Veränderungen des Herzens und der grossen Gefässe. Virchows Arch [Pathol Anat] 1921, 231:224–273
58. Karsner HT, Koletsky S: Calcific disease of the aortic valve. Philadelphia, J.B. Lippincott, 1947, p 43
59. Fishbein MC, Tan KS, Beazell JW, Schulman JH, Hirose FM, Criley JM: Cardiac pathology of transvenous pacemakers in dogs. Am Heart J 1977, 93:73–81
60. Van Vleet JF, Schollmeyer MP, Engle WR, Tacker WA Jr, Bourland JD: Cardiovascular alterations induced by chronic transvenous implantation of an automatic defibrillator electrode catheter in dogs. J Electrocardiol 1981, 14:67–72
61. Van Vleet JF, Tacker WA Jr, Bourland JD, Kallok MJ, Schollmeyer MP: Cardiac damage in dogs with chronically implanted automatic defibrillator electrode catheters and given 4 episodes of multiple shocks. Am Heart J, 1983, 106:300–307
62. Ayers KM, Jones SR: The cardiovascular system, Pathology of Laboratory Animals. Vol I. Edited by K Benirschke, FM Garner, TC Jones. New York, Springer-Verlag, 1978, pp 1–69
63. Liu S-K: Cardiac diseases in the dog and cat, Pig Model for Biomedical Research. Edited by HR Roberts, WJ Dodds. Pig Research Institute, Taiwan, Republic of China, 1982, pp 110–133
64. Rona G, Kahn DS: The healing of cardiac necrosis as reflected by experimental studies, Methods and Achievements in Experimental Pathology. Vol 3. Edited by E Bajusz, G Jasmin. Basel, S. Karger, 1967, pp 200–249
65. Bridges JB, Pritchard JJ: Bone and cartilage induction in rabbit. J Anat 1958, 92:28–38
66. Anderson KJ, Dingwall JA, Schmidt J, Le Cocq JF, Clawson DK: Induced connective tissue metaplasia: I. Heterogenous bone extract implants in the rat anterior eye chamber, a preliminary report. Transplant Bull 1960, 7:399–405
67. Groxatto OC: Producción experimental de cartílago en la aorta de perro: Relación con la medionecrosis quística de aorta humana. Medicina (Buenos Aires) 1953, 2:98–108
68. Rodbard S: Chondrogenesis induced in arteries by reduction in vascular extensibility. Fed Proc 1958, 17:134
69. Hommes FA, Van Leeuwen G, Zilliken F: Induction of cell differentiation: II. Isolation of a chondrogenic factor from embryonic chick spinal cords and notochords. Biochim Biophys Acta 1962, 56:320–325
70. McCandless EL, Lehoczky-Mona J, Rodbard S: Aortic cartilage produced by intramural carrageenan. Arch Pathol 1963, 75:507–516
71. Fishbein MC, Maclean D, Maroko PR: Experimental myocardial infarction in the rat; Qualitative and quantitative changes during pathologic evolution. Am J Pathol 1978, 90:57
72. Lehoczky-Mona J, McCandless EL: Ischemic induction of chondrogenesis in myocardium. Arch Pathol 1964, 78:37–42
73. Boyde A, Shapiro IM: Energy dispersive x-ray elemental analysis of isolated epiphyseal growth plate chondrocyte fragments. Histochemistry 1980, 69:85–94
74. Brighton CT, Hunt RM: Mitochondrial calcium and its role in calcification. Clin Orthop 1974, 100:406–416
75. Shapiro IM, Lee NH: The effect of oxygen, phosphoenolpyruvate and pH on the release of calcium from chondrocyte mitochondria. Metab Bone Dis Res 1978, 1:173–177
76. Brighton CT, Hepysenstall RB: Oxygen tension in epiphyseal plate, the metaphysis and diaphysis. J Bone Joint Surg 1971, 53A:719–728
77. Shapiro IM, Golub EE, Kakuta S, Hazelgrove J, Havery J, Chance B, Frasca P: Initiation of endochondral calcification is related to changes in redox state of hypertrophic chondrocytes. Science 1982, 217:950–952
78. Ham AW: A histological study of the early phases of bone repair. J Bone Joint Surg 1930, 12:827–844

Acknowledgments

We are grateful for the technical assistance of Mr. Thomas J. Nelson, the secretarial assistance of Ms. Pam McBride and Ms. Avis Morgan, and the inspiration and guidance given by the late Dr. Edward S. Reynolds.